Journal of Materials Chemistry C

Accepted Manuscript

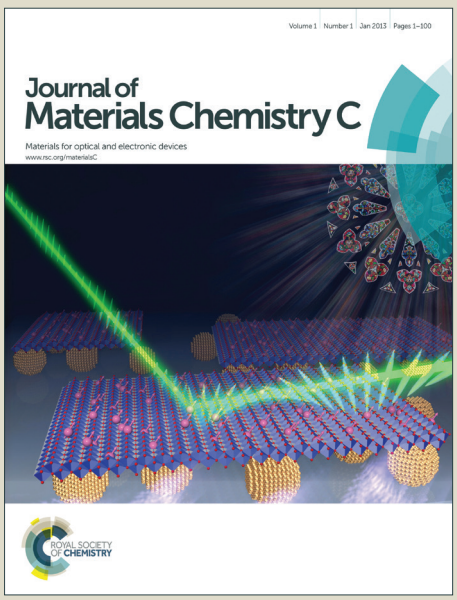

ROYAL SOCIETY OF CHEMISTRY

www.rsc.org/materialsC

A Light-Emitting Mechanism for Organic Light-Emitting Diodes: Molecular Design for Inverted Singlet-Triplet Structure and Symmetry-Controlled Thermally Activated Delayed Fluorescence *

Tohru Sato †[a,b], Motoyuki Uejima[a], Kazuyoshi Tanaka[a], Hironori Kaji[c], and Chihaya Adachi[d]

[a] Department of Molecular Engineering, Graduate School of Engineering, Kyoto University, Nishikyo-ku, Kyoto 615-8510, Japan

[b] Unit of Elements Strategy Initiative for Catalysts & Batteries, Kyoto University, Nishikyo-ku, Kyoto 615-8510, Japan

[c] Institute for Chemical Research, Kyoto University, Gokasho, Uji, Kyoto 611-0011, Japan

[d] Center for Organic Photonics and Electronics Research (OPERA), Kyushu University, 744 Motooka, Nishi, Fukuoka 819-0395, Japan

(Submitted on 30 October, 2013; Accepted on 2 November, 2014)

*Electronic supplementary information (ESI) available: (1) Selection rules; (2) Theory of vibronic coupling density; (3) Theory of transition dipole moment density; (4) Fundamental structure of anthracene derivatives; and (5) Vibronic coupling and transition dipole moment density analyses for pyrene **2** and its derivative **2a**.

†To whom correspondence should be addressed.

Fax: +81-75-383-2555; Tel: +81-75-383-2803; E-mail: tsato@moleng.kyoto-u.ac.jp

Abstract

The concepts of symmetry-controlled thermally activated delayed fluorescence (SC-TADF) and inverted singlet–triplet (iST) structure are proposed. Molecules that can exhibit SC-TADF or have an iST structure can be employed as a light-emitting molecule in organic light-emitting diodes. The molecular symmetry plays crucial roles in these concepts since they are based on the selection rules for the electric dipole transition, intersystem crossing, and nonradiative vibronic (electron–vibration) transitions. In addition to the symmetry conditions for the SC-TADF and iST molecules, the molecules should have small diagonal and off-diagonal vibronic coupling constants for suppressing vibrational relaxations and nonradiative vibronic transitions, respectively, and a large transition dipole moment for the fluorescence process. Analyses using the vibronic coupling and transition dipole moment densities are employed to reduce the vibronic coupling constants and to increase the transition dipole moment. The preferable point groups in the development of SC-TADF and iST molecules are discussed on the basis of the ratios of forbidden pairs of irreducible representations. It is found that the existence of the inversion symmetry is preferable for designing SC-TADF and iST molecules. On the basis of these guiding principles, we designed some anthracene and pyrene derivatives as candidate iST molecules. Their electronic structures, spin-orbit couplings, transition dipole moments, and vibronic couplings are discussed.

1 Introduction

In recent years, light-emitting molecules have been studied intensively because of their application for organic light-emitting diodes (OLEDs).[1–9] Although great progress has been made in the field of OLEDs, high external quantum yield (QY) of OLEDs remains a subject of great interest. According to spin statistics, singlet and triplet states are formed in a 1:3 ratio in exciton formations; therefore, the maximum internal QY is limited to 25% in fluorescence OLEDs.[10] Phosphorescence OLEDs[4,5] overcome this limitation by using mainly triplet excitons, but achieving both long operational lifetime and high efficiency remains difficult.[11–14] Significant advances, however, have been made in thermally activated delayed fluorescence (TADF) OLEDs,[15–20] which also utilise both triplet and singlet excitons[21].

The TADF molecules should have a small energy gap ΔE_{ST} between the first excited singlet S_1 and triplet T_1 states to enhance intersystem crossing (ISC) with thermal excitation. The small ΔE_{ST} can be achieved by reducing exchange integrals. For this reason, the TADF molecules are designed for a donor–acceptor system[16] so as to have a small overlap between the donor and acceptor.[15,22] However, there exists a trade-off between the reduction in exchange interactions and the enhancement of transition dipole moments (TDMs). To overcome this difficulty, one should pay attention to other types of TADF molecules. For example, Sn–porphins[15] and fullerenes[23–25] have been reported to be TADF molecules, although they are not donor–acceptor systems.

According to Kasha's rule, a light-emitting state is the lowest excited state because of the nonradiative transitions from the higher states.[26,27] For this reason, focus has usually been on the S_1 and T_1 states as light-emitting states. However, it is well known that there exist exceptions to Kasha's rule[28] (e.g., azulene[29]). The dominant fluorescence process of azulene is not the $S_1 \rightarrow S_0$ transition but the $S_2 \rightarrow S_0$ transition. Moreover, the photoluminescence quantum yield (PLQY) is not so small (being $\approx$20%),[30–32] which is ascribed to suppressions of the nonradiative decay $S_2 \rightarrow S_1$ caused by vibronic (electron–vibration) couplings.[32] This suggests that, as long as nonradiative vibronic transitions are suppressed, light emission from the higher excited state can be expected.

A high molecular symmetry reduces the number of active modes for vibronic couplings

between the higher and lower states because of their selection rules. Furthermore, if strengths of the vibronic couplings can be reduced as well as the number of them, nonradiative processes are suppressed because of weak vibronic couplings with the small number of active modes. Accordingly, we can expect light emission from the higher excited state.

Let us consider a fluorescent S_m state that lies energetically close to a triplet state T_n ($m \geq 1$, $n \geq 2$; see Fig. 1) from which the electric dipole transition to any lower triplet state $T_n \rightarrow T_k$ (for all k; $1 \leq k < n$) is symmetrically forbidden and from which the ISC $T_n \rightarrow S_m$ via spin-orbit coupling is symmetrically allowed. Fluorescence is assumed to be observed from the electric dipole transition from S_m to S_l ($m > l \geq 0$). In addition, from the view of efficiency, it is preferable that the ISC $S_m \rightarrow T_k$ is also assumed to be symmetrically forbidden. Under these conditions, the ISC $T_n \rightarrow S_m$ occurs before emissions from T_n. The T_n exciton generated by electric excitation can transform into the S_m exciton without undergoing a fluorescence process from T_n to T_k. It should be pointed out that the formation of T_n ($n > 1$) exciton is one of key issue, but recently Ma *et al.* have published the experimental evidence that the hot T_n excitons are generated in the PTZ–BZP OLED[33].

The energy gap between S_m and T_n is simply denoted as $\Delta E_{ST} = E_{S_m} - E_{T_n}$. It should be noted that, in the literature on TADF OLEDs, ΔE_{ST} means the energy gap between S_1 and T_1.[16–18] If ΔE_{ST} is positive and small, TADF from the S_m exciton via the T_n exciton with thermal excitation can be expected irrespective of the values of the subscripts m and n. High molecular symmetry can prohibit undesirable transitions, which results in fluorescence even if the ΔE_{ST} between S_1 and T_1 is somewhat larger than that for conventional TADF. We call this new type of TADF a symmetry controlled TADF (SC-TADF). One of the advantages of this approach is that the candidates are not restricted to donor–acceptor systems. Therefore, we can overcome the trade-off between the reduction in exchange interactions and the enhancement of TDMs.

In contrast, if ΔE_{ST} is negative, triplet excitons can transform into singlet ones without thermal excitation. We call the electronic structure with a negative ΔE_{ST} an inverted singlet-triplet (iST) structure. Contrary to the TADF molecules of the donor–acceptor type, SC-TADF or iST molecules can have a large TDM between the S_m and S_l states. However, the TDM of a

TADF molecule based on the donor–acceptor model[16] is inevitably small, because of the small overlap density between S_1 and S_0 to reduce the exchange integral and, therefore, the small ΔE_{ST}. In this article, we report the principle for designing SC-TADF and iST molecules based on selection rules and apply it to the anthracene and pyrene derivatives shown in Fig. 2.

In addition to use of selection rules, the suppression of vibrational relaxations and nonradiative vibronic transitions $S_m \rightarrow S_l$ and $T_n \rightarrow T_k$ is required. Large vibrational relaxations cause small Franck–Condon factors, which lead to suppression of radiative transitions. Strong internal conversions can lower PLQY and ELQY. The vibrational relaxations and internal conversions are caused by vibronic couplings[34,35] or electron–phonon couplings, and their magnitudes are given by vibronic coupling constants (VCCs). Even if the selection rules are fully employed, there always exist vibronically active modes such as totally symmetric modes for diagonal VCCs. Therefore, vibrational relaxation and nonradiative vibronic transitions via such active modes should be suppressed as much as possible. In other words, the VCCs should be reduced as well as the number of active modes. The VCCs can be analysed in terms of the vibronic coupling density (VCD).[36–38] The TDM, which is a factor in the fluorescence rate, can be represented in density form as the transition dipole moment density (TDMD).[39] We have successfully applied the VCD and TDMD analyses to anthracene chlorides to explain their PLQYs[40]. Therefore, the validity of these analyses have been confirmed. The combination of the VCD and TDMD analyses helps us to reduce VCCs and increase TDMs, respectively. We have succeeded in controlling the VCCs and TDMs using VCD and TDMD analyses: PLQY for **1b** (see Fig. 2) was measured to be 96%.[41] As examples of the VCD and TDMD analyses, we discuss **2** and **2a** (see Fig. 2) in the Electronic Supplementary Information (ESI).

In this article, we present a principle for designing SC-TADF and iST structures by considering symmetry and using VCD and TDMD analyses. We designed anthracene and pyrene derivatives **1a**–**1c** and **2a**–**2e** as iST molecules (Fig. 2). In Section 2.1, we present the selection rules for electric transition dipole moment and spin-orbit coupling. The preferable point groups are discussed in Section 2.2, with a focus on the selection rule of the D_{2h} point group. The selection rules of the point groups D_{3h} and D_{4h} are mentioned in Section S1 of the ESI. The VCD and TDMD concepts are described in Sections S2 and S3 of the ESI, respectively. The

calculation methods are described in Section 3. The electronic structures of these candidates are discussed in Section 4.1 for the anthracene derivatives and in Section 4.2 for the pyrene derivatives. The definition of fundamental structure is given in Section S4 of the ESI. The VCD and TDMD analyses for pyrene **2** and its derivative **2a** are expounded in Section S5 of the ESI. Their oscillator strengths are discussed in Section 4.3. We summarise the present study in Section 5.

2 Theory

2.1 Selection rules

For simplicity, we assume that $l = 0$, $m = k = 1$, and $n = 2$, hereafter. We denote singlet wavefunctions as Ψ_{S_0}, Ψ_{S_1} and triplet wavefunctions as Ψ_{T_1}, Ψ_{T_2}. They belong to Γ_{S_0}, Γ_{S_1}, Γ_{T_1}, and Γ_{T_2} irreps, respectively.

The TDM is given by

$$\boldsymbol{\mu}_{S_1 \to S_0} = \langle \Psi_{S_1} | \hat{\boldsymbol{\mu}} | \Psi_{S_0} \rangle, \tag{1}$$

where $\hat{\boldsymbol{\mu}}$ is the electric dipole moment operator. The TDM between the T_2 and T_1 states is also defined by the same expression as Eq. (1).

We consider the one-electron term of the spin-orbit coupling as the origin of the ISC.[42] The spin-orbit integral is defined by the matrix element of the one-electron part of the effective spin-orbit coupling operator $\hat{H}_{SO}$:

$$\zeta_{S_1 \to T_2} = \langle \Psi_{T_2} | \hat{H}_{SO} | \Psi_{S_1} \rangle. \tag{2}$$

The symmetry for the orbital part of the operator $\hat{H}_{SO}$ is governed by the symmetry of orbital angular momentum $\hat{\boldsymbol{l}}$. An ISC is forbidden if the matrix element of the orbital angular momentum $\hat{\boldsymbol{l}}$ is equal to zero. Because the one-electron operators of the electric dipole moment $\boldsymbol{\mu}$ and orbital angular momentum $\hat{\boldsymbol{l}}$ are tensor operators of rank one, or vector operators, we can derive their selection rules based on their irreps: If initial and final states belong to Γ_1 and Γ_2 irreps, respectively, and a tensor operator belongs to Γ_3 irrep, and if the inclusion relation[43]

$$\Gamma_2 \in \Gamma_3 \times \Gamma_1 \tag{3}$$

holds, the transition between Γ_1 and Γ_2 states is allowed; otherwise, the transition is forbidden. For the electric dipole and spin-orbit interactions, we will discuss the allowed or forbidden pairs of irreps for some point groups later.

In addition to the electric dipole and spin-orbit couplings we discuss the selection rule for the vibronic coupling. The diagonal VCC is defined by

$$V_{1,\alpha} = \left\langle \Psi_{S_1} \middle| \hat{V}_\alpha \middle| \Psi_{S_1} \right\rangle, \tag{4}$$

where $\hat{V}_\alpha$ denotes the electronic part of the vibronic coupling operator of normal mode α that belongs Γ_3 irrep. The off-diagonal VCC is defined by

$$V_{10,\alpha} = \left\langle \Psi_{S_0} \middle| \hat{V}_\alpha \middle| \Psi_{S_1} \right\rangle, \tag{5}$$

The VCC between the triplet states is also defined by Eq. (5). All the VCCs between the single and triplet states are zero. The diagonal VCC $V_{1,\alpha}$ gives rise to vibrational relaxation in the S_1 state. The off-diagonal VCC $V_{10,\alpha}$ is a factor of the rate constant of the internal conversion $S_1 \rightarrow S_0$. In the case of $\Gamma_2 \in \Gamma_3 \times \Gamma_1$, the Γ_3 mode is active in vibronic couplings, and nonradiative vibronic decay via the Γ_3 mode is allowed between the electronic states Γ_1 and Γ_2. The vibronic transition is not completely forbidden in any molecule because the active Γ_3 mode always exists. In other words, a nonradiative vibronic transition is inevitable. However, the number of active modes can be suppressed by designing a highly symmetric molecule. Moreover, the concept of vibronic coupling density enables us to reduce the VCCs of the active modes with an appropriate molecular design. We will discuss the application of the vibronic coupling density later.

2.2 Point group symmetry

Point group symmetry is crucial for an iST structure and SC-TADF. From the viewpoint of molecular design, we can easily design iST or SC-TADF molecules if a forbidden pair of (Γ_1, Γ_2) frequently appear in all possible pairs of irreps. In this subsection, we discuss the ratio of the forbidden pairs (Γ_1, Γ_2) for the electric dipole transition and the spin-orbit coupling.

As an example, we focus on the selection rules of the D_{2h} point group. The character table for D_{2h} is shown in Table S1[44]. The position operator components $\hat{x}$, $\hat{y}$, and $\hat{z}$ belong to B_{3u}, B_{2u}, and B_{1u}, respectively. The electric dipole moment operator components are the same irreps

because they are proportional to the position operators. If the initial state is a totally symmetric representation $\Gamma_1 = A_g$, the direct products $\Gamma_3 \times \Gamma_1$ are decomposed as follows:

$$B_{3u} \times A_g = B_{3u}, \quad B_{2u} \times A_g = B_{2u}, \quad B_{1u} \times A_g = B_{1u}. \tag{6}$$

Hence, the radiative transition via electric dipole coupling from the initial A_g state is allowed when the final state is B_{3u}, B_{2u}, or B_{1u}. The selection rule is summarised in Table 1.

The orbital angular momentum operator components $\hat{l}_x$, $\hat{l}_y$, and $\hat{l}_z$ belong to B_{3g}, B_{2g}, and B_{1g}, respectively. If the initial state is $\Gamma_1 = B_{1u}$, the direct products between the irreps of the components of the orbital angular momentum, Γ_3, and that of the final state, Γ_2, are given as follows:

$$B_{3g} \times B_{1u} = B_{2u}, \quad B_{2g} \times B_{1u} = B_{3u}, \quad B_{1g} \times B_{1u} = A_u. \tag{7}$$

The selection rule for the spin-orbit coupling is summarised in Table 2.

Since the number of conjugacy classes, n_c is equal to the number of irreps, n_r,[43] the total number of all possible irrep pairs is equal to $n_r^2 = n_c^2$. For the D_{2h} point group, $n_c = 8$. As shown in Tables 1 and 2, the number of forbidden pairs, n_f, or the number of "×" s, is 40. Therefore, the ratio of the forbidden pairs, n_f/n_c^2, is 62.5% (40 out of 64). It should be noted that inversion symmetry plays an important role. According to the Laporté rule,[45] the electric dipole transition is forbidden when both Γ_1 and Γ_2 are gerade (g) or ungerade (u). Therefore, half of the irrep pairs (Γ_1, Γ_2) are at least forbidden if the point group has inversion symmetry. Similarly, if the irrep pair (Γ_1, Γ_2) is (u, g) or (g, u), the matrix element of the orbital angular momentum is zero. For this reason, the ratio of the forbidden pairs for spin-orbit coupling is also over 50% in the point group with inversion symmetry. The selection rules for D_{3h} and D_{4h} are described in the ESI.

The ratios of forbidden pairs and the numbers of elements (order), n_g, are tabulated in Table 3. The order of the ratios is as follows:

$$D_{6h} > O_h > I_h = D_{4h} > D_{2h} > D_{3h} > T_d > C_i = C_{2h} > D_{2d} = C_{4v} > D_2 = C_{2v} > C_{3v} > C_s = C_1. \tag{8}$$

Note that this series is not the same as the order of n_g. This series suggests that it is no accident that the TADF molecule C_{60}[23] has I_h symmetry and that the Sn–porphins[15] are nearly D_{4h}.

In other words, they can be SC-TADF molecules. Molecules with the high symmetry of D_{6h}, O_h, I_h, D_{4h}, D_{2h}, and so on are good candidates for iST and SC-TADF molecules. This series indicates the meaning of *high* symmetry in the present problem.

3 Calculation Method

We designed anthracene derivatives **1a**–**1c** and pyrene derivatives **2a**–**2e** with D_{2h} symmetry (see Fig. 2). The anthracene, pyrene, and their derivatives were optimised for the S_0 state and the stability of their structures were confirmed by using vibrational analyses. The calculations were based on the B3LYP/6-31G(d,p) level of theory. Then, excited singlet and triplet states were obtained by employing TD-B3LYP/6-31G(d,p) calculations. These calculations were carried out by using the Gaussian 09 program.[46] The spin-orbit coupling integrals were calculated using the effective nuclear charge[47,48] with our code. The vibronic coupling constant, vibronic coupling density, electron-density difference, and overlap density were also obtained with our program.

4 Results and Discussion

4.1 Anthracene and its derivatives

Prior to the designed molecules, we discuss anthracene **1**. Energy levels of **1** are shown in Fig. 3 (a). The energy levels for the S_1, T_1, T_2, and T_3 states are 1.804, 3.274, 3.299, and 3.509, in eV. The energy level for the T_1 state is much lower than that for the S_1 state. The energy gap between S_1 and T_2 is negative but the ISC between them is forbidden. The energy gap between S_1 and T_3 is equal to -0.2345 eV and the spin-orbit integral is 0.27 cm^{-1} (0.033 meV). Since the electric dipole transition from T_3 to T_2 is allowed, the T_3 exciton can make a transition to the T_2 state, and the molecule in the T_2 state can fluoresce to the T_1 state. In addition, the molecule in the T_2 state can undergo nonradiative vibronic transitions. The spin-orbit coupling $T_2 \rightarrow S_1$ is forbidden so that the ISC $T_2 \rightarrow S_1$ and phosphorescence $T_2 \rightarrow S_0$ are probably very weak. Thus, anthracene **1** is neither an iST molecule nor an SC-TADF molecule.

We have already designed and reported anthracene derivative **1a** as a highly efficient fluorescence molecule.[41] Molecule **1a** was designed by using VCD and TDMD analyses to suppress vibronic coupling and enhance radiative transition. Molecule **1a** was synthesised, and high photoluminescence quantum yield (PLQY = 96%) was observed in solution. Here we discuss the iST structure of **1a**. The energy levels of anthracene derivative **1a** are shown in Fig. 3 (b). The energy levels for the S_1, T_1, and T_2 states are 2.304, 1.244, and 2.345, in eV. The energy level for the S_1 state indicates green fluorescence. The energy level for the T_1 state is much lower than that for the S_1 state. The energy gap between S_1 and T_2 is negative and the ISC between them is allowed. In addition, the electric dipole transition between T_2 and T_1 is forbidden. Because the electric dipole transition $T_2 \rightarrow T_1$ is forbidden, the nonradiative vibronic transitions from S_1 is suppressed, and the radiative transition $S_1 \rightarrow S_0$ is enhanced in the molecular design of **1a**,[41] the T_2 exciton can be converted into the S_1 state without thermal excitation, and the S_1 state can fluoresce. Therefore, **1a** can be categorised as an iST molecule.

Molecules **1b** and **1c** were designed for solubility. Their symmetries are lowered because of the alkyl substitutions, and, therefore, the selection rules are broken in the strict sense; the point groups for **1b** and **1c** are C_1 and C_{2h}, respectively. The energy levels of **1b** and **1c** are shown in Fig. 4. It is found that the energy levels of **1b** and **1c** are not so different from those of **1a**. Figure 4a shows that all the transitions in **1b** become allowed. For **1c**, in contrast, the spin-orbit coupling between S_1 and T_1 becomes allowed, and the electric dipole transitions from S_2 to S_1 and from T_2 to T_1 are still forbidden (Fig. 4b). However, comparing the electronic structures of **1b** and **1c** with that of **1a**, one sees that the alkyl substitutions do not affect their electronic states so much that **1b** and **1c** keep their transition probabilities in spite of the symmetry breaking. The transition probabilities corresponding to the forbidden transitions in **1a** are almost zero (see Fig. 3 (b)): For molecule **1c**, the TDM of the electric dipole transition from T_2 to T_1 is 1.18×10^{-6} a.u., and that from S_2 to S_1 is 1.12×10^{-6} a.u.; the spin-orbit integral between S_1 and T_1 is 0.008 cm^{-1}. The spin-orbit integrals between $T_2 \rightarrow S_1$ and TDMs of **1b** and **1c** are almost the same as those of **1a**. This is because the electronic states are not changed by the alkyl groups. Therefore, molecules **1b** and **1c** can also be expected to be iST molecules.

We define a *fundamental structure*, as the molecular structure that has higher symmetry

than the original structures (see Section S4 of the ESI). As long as the electronic structure of the symmetric fundamental structure is almost maintained against modifications, for example by adding substituents, the molecule can be categorised as an SC-TADF or an iST molecule. This is because the relevant transition probabilities are little affected by the modifications.

4.2 Pyrene and its derivatives

Pyrene **2**, of which point group is D_{2h}, and its derivatives[49–52] are also fluorescent molecules. Pyrene derivatives **2a**–**2e** are examined to determine whether they are iST molecules. The nonradiative decays cannot be completely suppressed, even if the symmetry of the molecule is high. There remain some vibronically active modes. These pyrene derivatives were designed to have small VCCs and large TDM. The reason why they have the suppressed VCCs and enhanced TDM is expounded in the Section S5 of the ESI, with a focus on pyrene **2** and its derivative **2a**. The energy levels of pyrene **2** are shown in Fig. 5. The energy levels of the S_1, T_1–T_4 states are 3.718, 2.123, 3.463, 3.569, and 3.617, respectively, in eV. The T_1–T_4 levels are lower than the S_1 state. Though the spin-orbit integral between T_2 and S_1 is allowed and the electric dipole transitions $T_4 \rightarrow T_3$ and $T_3 \rightarrow T_2$ are allowed, $T_2 \rightarrow T_1$ is forbidden. It is found that the energy gap between the S_1 and T_2 states is large for thermal activation. Therefore, pyrene **2** is not an iST molecule nor an SC-TADF molecule.

The energy levels for the pyrene derivative **2a** are shown in Fig. 6a. The energy levels for S_1, T_1, T_2, and T_3 states are 2.520, 1.474, 2.767, and 2.804, in eV. The energy gap ΔE_{ST} between S_1 and T_2 has a negative value of -0.247 eV, and the ISC $T_2 \rightarrow S_1$ is allowed. The electric dipole transition $T_2 \rightarrow T_1$ is forbidden. Therefore, **2a** is an iST molecule. However, T_3 is close to T_2 with a small energy gap of 0.037 eV, and the electric dipole transition from T_3 to T_1 is allowed. Therefore, in electric excitation, T_3 excitons as well as the T_2 excitons can be generated, and the T_2 exciton can also make a thermal excitation to the T_3 state, which can give rise to fluorescence and nonradiative vibronic transitions. The processes discussed above would be faster than the ISC, with the rate of the ISC being small in spite of the negative energy gap of ΔE_{ST}. Accordingly, we cannot expect **2a** to be an iST molecule.

We designed **2b** to enlarge the energy gap between the T_2 and T_3 states of **2a**. To make

the energy levels of T_2 and S_1 of **2a** closer and to increase the energy difference between T_2 and T_3 of **2a**, we introduce two fluorine atoms into **2a** because the pseudodegeneracy in **2a** originates from weak interaction between the four 1-pyrrolylethynyl groups. As the result, the energy levels of the S_1, T_2, and T_3 states become 2.481, 2.564, and 2.757, in eV, respectively. The energy gap ΔE_{ST} between S_1 and T_2 becomes narrower in **2b** than **2a**, as shown in Fig. 6b; the value of ΔE_{ST} for **2b** is equal to -0.083 eV. Therefore, **2b** can be an iST molecule.

The energy levels for pyrene derivative **2c** are shown in Fig. 7. As is the case in **2a**, **2c** is not identified as an iST molecule because of the forbidden $T_2 \rightarrow S_1$ transition. In addition, T_2 and T_3 excitons are generated with nearly equal probability because of their pseudodegeneracy (T_2 2.519 eV; T_3 2.530 eV). The T_2 exciton cannot be transformed into an S_1 exciton because the ISC $T_2 \rightarrow S_1$ is forbidden. Therefore, the T_2 exciton can give rise to the electric dipole transition $T_2 \rightarrow T_1$ as well as nonradiative vibronic transitions. For pyrene derivative **2c**, 1,3,6,8-tetrakis(phenylethynyl)pyrene, its synthesis and PLQY measurement (99%) have been already reported.[50,52] The high PLQY can be ascribed to the small off-diagonal VCCs and the large TDM, as discussed for **2a** in the ESI.

The energy levels of **2d** and **2e**, which are also fluorinated molecules, are shown in Fig. 8. The energy levels between the T_2 and T_3 states are large enough in both **2d** and **2e** to avoid the generation of the T_3 exciton in electric excitation and in the thermal excitation from T_2 to T_3. The transitions $T_2 \rightarrow S_1$ are allowed with negative ΔE_{ST}. In addition, the electric dipole transitions $T_2 \rightarrow T_1$ are forbidden. Hence, **2d** and **2e** are categorised as iST molecules. As is not the case in **2c**, the T_2 exciton of **2d** and **2e** can be generated selectively because they have large energy gaps between the T_2 and T_3 states.

The efficient formation of T_2 or T_n exciton is crucial in the iST and SC-TADF mechanism. If the T_2 or T_n states cannot be formed in OLEDs, the T_1 exciton could give rise to nonradiative decay. Therefore, the device design for the formation T_n $(n > 1)$ exciton, for example, tuning of orbital levels of host materials in an emitting layer, would be important to realize highly efficient OLED using the iST and SC-TADF mechanism.

4.3 Oscillator strength

The values of oscillator strengths f between the S_1 and S_0 states and energy gaps ΔE_{ST} between the T_2 and S_1 states are summarised in Table 4. It is found that **1a**, **1b**, **1c**, **2b**, **2d**, and **2e** have large f values and negative ΔE_{ST} within 0.1 eV and preferable electronic structures. Hence, they are good candidates for iST molecules.

5 Conclusion

We have proposed symmetry-controlled thermally activated delayed fluorescence (SC-TADF) and inverted singlet-triplet (iST) structure. The advantage of the iST and SC-TADF concepts is that they can extend the scope for the molecular design other than the donor–acceptor systems. The design principles for SC-TADF and iST molecules are as follows:

1. The electric dipole transition between the S_m and S_l states is symmetrically allowed,
2. spin-orbit coupling between the T_n and S_m states is symmetrically allowed, and
3. the electric dipole transition between the T_n and T_k states is symmetrically forbidden,

where each of l, m, and n is a certain integer satisfying $m \geq 1$, $n \geq 2$, and $m > l \geq 0$. Note that k is all the natural numbers satisfying $1 \leq k < n$. Moreover, to increase the quantum yield, it is preferable that the spin-orbit coupling between the T_k and S_m states be symmetrically forbidden. These processes compete with nonradiative vibronic transitions $S_m \rightarrow S_l$ and $T_n \rightarrow T_k$. Though they are inevitable in a molecule, the number of active modes can be reduced in a highly symmetric molecule. Moreover, we can suppress nonradiative vibronic transitions by reducing the off-diagonal vibronic coupling constants of the remaining active modes. To reduce vibronic couplings we have used a vibronic coupling density analysis. In addition, to increase the transition dipole moments between the S_m and S_l states, we have employed the transition dipole moment density concept. The molecules **1a**, **2b**, **2d**, and **2e** satisfy all the conditions above.

Even if molecular symmetry is low, the molecule can be categorised as an SC-TADF or an iST molecule, as long as the fundamental structure, defined as a subunit of the molecule where

the electron density difference $\Delta\rho_m$ and the overlap density ρ_{ml} are mostly localised, satisfies the above conditions. By analysing $\Delta\rho_m$ and ρ_{ml}, we have found that the alkyl substitutions to the anthracene derivative **1a** do not affect the electronic structures as much compared with the fundamental structure. Therefore they do not change the transition probabilities so much. Hence, **1b** and **1c** are also expected to exhibit almost similar fluorescence properties to **1a**.

From the viewpoint of molecular design, inversion symmetry is important because of the Laporté rule. The preferable point groups are D_{6h}, O_h, I_h, D_{4h}, D_{2h}, and so on because they have a high ratio of forbidden irrep pairs for electric dipole transition and spin-orbit coupling.

From our preliminary calculations on C_{60} and Sn-porphins, we have found that they can be SC-TADF molecules. Molecule **1a** has already been observed as a highly efficient fluorescent molecule in solution (PLQY = 96%). The measurement of its ELQY is under investigation. Syntheses of the other candidates (**2b**, **2d**, and **2e**) are also in progress. These results will be published in the near future.

Acknowledgments

Numerical calculations were performed partly at the Supercomputer Laboratory of Kyoto University and at the Research Center for Computational Science, Okazaki, Japan. This research was supported by the Japan Society for the Promotion of Science (JSPS) through its Funding Program for World-Leading Innovative R&D on Science and Technology (FIRST Program). This work was also supported by a Grant-in-Aid for Scientific Research (C) (24550210) from JSPS.

References

[1] C. W. Tang and S. A. VanSlyke, *Appl. Phys. Lett.*, 1987, **51**, 913.

[2] C. Adachi, T. Tsutsui and S. Saito, *Appl. Phys. Lett.*, 1989, **55**, 1489.

[3] R. H. Friend, R. W. Gymer, A. B. Holmes, J. H. Burroughes, R. N. Marks, C. Taliani, D. D. C. Bradley, D. A. D. Santos, J. L. Brédas, M. Löglund and W. R. Salaneck, *Nature*, 1999, **397**, 121.

[4] M. A. Baldo, S. Lamansky, P. E. . Burrows and M. E. Thomson, *Appl. Phys. Lett.*, 1999, **75**, 4.

[5] M. A. Baldo, M. E. Thompson and S. R. Forrest, *Nature*, 2000, **403**, 750.

[6] L. S. Hung and C. H. Chen, *Mater. Sci. Eng. R*, 2002, **39**, 143.

[7] B. W. D'Andrade and S. R. Forrest, *Adv. Mater.*, 2004, **16**, 1585.

[8] C. C. Wu, Y. T. Lin, K. T. Wong, R. T. Chen and Y. Y. Chien, *Adv. Mater.*, 2004, **16**, 61.

[9] R. J. Tseng, R. C. Chiechi, F. Wudl and Y. Yang, *Appl. Phys. Lett.*, 2006, **88**, 093512.

[10] V. Cleave, G. Yahioglu, P. L. Barny, R. H. Friend and N. Tessler, *Adv. Mater.*, 1999, **11**, 285.

[11] T.-H. Su, C.-H. Fan, Y.-H. Ou-Yang, L.-C. Hsu and C.-H. Cheng, *J. Mater. Chem. C*, 2013, **1**, 5084–5092.

[12] R. C. Kwong, M. R. Nugent, L. Michalski, T. Ngo, K. Rajan, Y.-J. Tung, M. S. Weaver, T. X. Zhou, M. Hack, M. E. Thompson, S. R. Forrest and J. J. Brown, *Appl. Phys. Lett.*, 2002, **81**, 162.

[13] R. Meerheim, K. Walzer, M. Pfeiffer and K. Leo, *Appl. Phys. Lett.*, 2006, **89**, 061111.

[14] T. Tsuzuki and S. Tokito, *Appl. Phys. Lett.*, 2009, **94**, 033302.

[15] A. Endo, M. Ogasawara, A. Takahashi, D. Yokoyama, Y. Kato and C. Adachi, *Adv. Mater.*, 2009, **21**, 4802–4086.

[16] A. Endo, K. Sato, K. Yoshimura, T. Kai, A. Kawada, H. Miyazak and C. Adachi, *Appl. Phys. Lett.*, 2011, **98**, 083302.

[17] T. Nakagawa, S.-Y. Ku, K.-T. Wong and C. Adachi, *Chem. Comm.*, 2012, **48**, 9580–9582.

[18] H. Uoyama, K. Goushi, K. Shizu, H. Nakamura and C. Adachi, *Nature*, 2012, **492**, 234–240.

[19] C. Adachi, *Jpn. J. Appl. Phys.*, 2014, **53**, 060101 1–11.

[20] Y. Tao, K. Yuan, T. Chen, P. Xu, H. Li, R. Chen, C. Zheng, L. Zhang and W. Huang, *Adv. Mater.*, 2014, 1–28.

[21] B. Valeur, in *Molecular Fluorescence*, Wiley-VCH, Weinheim, 2002, vol. 158, p. 41.

[22] N. J. Turro, *Modern Molecular Photochemistry*, University Science Books, Sausalito, CA, 1991.

[23] F. A. Salazar, A. Fedorov and M. N. Berberan-Santos, *Chem. Phys. Lett.*, 1997, **271**, 361–366.

[24] S. M. Bachilo, A. F. Benedetto, R. B. Weisman, J. R. Nossal and W. E. Billups, *J. Phys. Chem. A*, 2000, **104**, 11265–11269.

[25] C. Baleizão and M. N. Berberan-Santos, *Ann. N.Y. Acad. Sci.*, 2008, **1130**, 224–234.

[26] M. Kasha, *Discussion Faraday Soc.*, 1950, **9**, 14–19.

[27] M. Kasha, *Radiation Res. Suppl.*, 1960, **2**, 243.

[28] T. Itoh, *Chem. Rev.*, 2012, **112**, 4541–4568.

[29] M. Beer and H. C. Longuet-Higgins, *J. Chem. Phys.*, 1955, **23**, 1390.

[30] I. Berlman, *Handbook of fluorescence spectra of aromatic molecules*, Academic Press, New York, 1965.

[31] J. Birks, *Photophysics of aromatic molecules*, Wiely, New York, 1970.

[32] S. Murata, C. Iwanaga and H. Kokubun, *Chem. Phys. Lett.*, 1972, **13**, 101–104.

[33] L. Yao, S. Zhang, R. Wang, W. Li, F. Shen, B. Yang and Y. Ma, *Angew. Chem.*, 2014, **126**, 2151–2155.

[34] G. Fischer, *Vibronic Coupling: The Interaction Between the Electronic and Nuclear Motions*, Academic Press, London, 1984.

[35] I. B. Bersuker and V. Z. Polinger, *Vibronic Interactions in Molecules and Crystals*, Springer–Verlag, Berlin and Heidelberg, 1989.

[36] T. Sato, K. Tokunaga and K. Tanaka, *J. Phys. Chem. A*, 2008, **112**, 758.

[37] T. Sato, K. Shizu, T. Kuga, K. Tanaka and H. Kaji, *Chem. Phys. Lett.*, 2008, **458**, 152.

[38] T. Sato, K. Tokunaga, N. Iwahara, K. Shizu and K. Tanaka, in *The Jahn–Teller Effect: Fundamentals and Implications for Physics and Chemistry*, ed. H. Köppel, D. R. Yarkony and H. Barentzen, Springer–Verlag, Berlin and Heidelberg, 2009, p. 99.

[39] T. Sato, M. Uejima, N. Iwahara, N. Haruta, K. Shizu and K. Tanaka, *J. Phys.: Conf. Ser.*, 2013, **428**, 012010.

[40] M. Uejima, T. Sato, K. Tanaka and H. Kaji, *Chem. Phys.*, 2014, **430**, 47–55.

[41] M. Uejima, T. Sato, M. Detani, A. Wakamiya, F. Suzuki, H. Suzuki, T. Fukushima, K. Tanaka, Y. Murata, C. Adachi and H. Kaji, *Chem. Phys. Lett.*, 2014, **602**, 80–83.

[42] S. I. Lower and M. A. El-Sayed, *Chem. Rev.*, 1966, **66**, 199–241.

[43] M. Hamermesh, *Group Theory and Its Application to Physical Problems*, Dover Publications, New York, 1962.

[44] S. L. Altmann and P. Herzig, *Point Group Theory Tables*, Clarendon, Oxford, 1994.

[45] O. Laporte and W. F. Meggers, *J. Opt. Am. Soc.*, 1925, **11**, 459–460.

[46] M. J. Frisch, G. W. Trucks, H. B. Schlegel, G. E. Scuseria, M. A. Robb, J. R. Cheeseman, G. Scalmani, V. Barone, B. Mennucci, G. A. Petersson, H. Nakatsuji, M. Caricato, X. Li, H. P. Hratchian, A. F. Izmaylov, J. Bloino, G. Zheng, J. L. Sonnenberg, M. Hada, M. Ehara, K. Toyota, R. Fukuda, J. Hasegawa, M. Ishida, T. Nakajima, Y. Honda, O. Kitao, H. Nakai, T. Vreven, J. A. Montgomery, Jr., J. E. Peralta, F. Ogliaro, M. Bearpark, J. J. Heyd, E. Brothers, K. N. Kudin, V. N. Staroverov, R. Kobayashi, J. Normand, K. Raghavachari, A. Rendell, J. C. Burant, S. S. Iyengar, J. Tomasi, M. Cossi, N. Rega, J. M. Millam, M. Klene, J. E. Knox, J. B. Cross, V. Bakken, C. Adamo, J. Jaramillo, R. Gomperts, R. E. Stratmann, O. Yazyev, A. J. Austin, R. Cammi, C. Pomelli, J. W. Ochterski, R. L. Martin, K. Morokuma, V. G. Zakrzewski, G. A. Voth, P. Salvador, J. J. Dannenberg, S. Dapprich, A. D. Daniels, Ö. Farkas, J. B. Foresman, J. V. Ortiz, J. Cioslowski and D. J. Fox, *Gaussian 09 Revision B.1*, Gaussian, Inc., Wallingford, CT, 2009.

[47] S. R. Langhoff, *J. Chem. Phys.*, 1980, **73**, 2379–2386.

[48] S. Koseki, M. S. Gordon, M. W. Schmidt and N. Matsunaga, *J. Phys. Chem.*, 1995, **99**, 12764–12772.

[49] B.-C. Wang, J.-C. Chang, H.-C. Tso, H.-F. Hsu and C.-Y. Cheng, *Journal of Molecular Structure: THEOCHEM*, 2003, **629**, 11–20.

[50] A. Hayer, V. de Halleux, A. Köhler, A. El-Garoughy, E. W. Meijer, J. Barberá, J. Tant, J. Levin, M. Lehmann, J. Gierschner, J. Cornil and Y. H. Geerts, *J. Phys. Chem. B*, 2006, **110**, 7653–7659.

[51] Y. H. Park, H. H. Rho, N. G. Park and Y. S. Kim, *Current Applied Physics*, 2006, **6**, 691–694.

[52] K. Fujimoto, H. Shimizu, M. Furusyo, S. Akiyama, M. Ishida, U. Furukawa, T. Yokoo and M. Inouye, *Tetrahedron*, 2009, **65**, 9357–9361.

Table 1: Selection rule for the electric dipole moment operator in D_{2h} symmetry. Entries of x, y, and z mean that the component of electric dipole transition is allowed. The notation $\times$ indicates a forbidden irreps pair.

	A_g	B_{1g}	B_{2g}	B_{3g}	A_u	B_{1u}	B_{2u}	B_{3u}
A_g	$\times$	$\times$	$\times$	$\times$	$\times$	z	y	x
B_{1g}		$\times$	$\times$	$\times$	z	$\times$	x	y
B_{2g}			$\times$	$\times$	y	x	$\times$	z
B_{3g}				$\times$	x	y	z	$\times$
A_u					$\times$	$\times$	$\times$	$\times$
B_{1u}						$\times$	$\times$	$\times$
B_{2u}							$\times$	$\times$
B_{3u}								$\times$

Table 2: Selection rule for the orbital angular momentum operator $\hat{\boldsymbol{l}}$ in D_{2h} symmetry. Entries of l_x, l_y, and l_z indicate the nonzero component of $\hat{\boldsymbol{l}}$. The notation $\times$ indicates a forbidden irreps pair.

	A_g	B_{1g}	B_{2g}	B_{3g}	A_u	B_{1u}	B_{2u}	B_{3u}
A_g	$\times$	l_z	l_y	l_x	$\times$	$\times$	$\times$	$\times$
B_{1g}		$\times$	l_x	l_y	$\times$	$\times$	$\times$	$\times$
B_{2g}			$\times$	l_z	$\times$	$\times$	$\times$	$\times$
B_{3g}				$\times$	$\times$	$\times$	$\times$	$\times$
A_u					$\times$	l_z	l_y	l_x
B_{1u}						$\times$	l_x	l_y
B_{2u}							$\times$	l_z
B_{3u}								$\times$

Table 3: Order (the number of elements) of the point group, n_g, the number of the conjugacy classes, n_c, the number of the forbidden electric dipole transitions and intersystem crossings, n_f, and ratio of the forbidden irreps pair to all of the irreps pairs.

Point group	n_g	n_c	n_f	Ratio ($= n_f/n_c^2$) (%)
C_s	2	2	0	0
C_i	2	2	2	50
C_{2h}	4	4	8	50
C_{2v}	4	4	4	25
C_{3v}	6	3	2	22.2
C_{4v}	8	5	12	48
D_2	4	4	4	25
D_{2d}	8	5	12	48
D_{2h}	8	8	40	62.5
D_{3h}	12	6	20	55.6
D_{4h}	16	10	74	74
D_{6h}	24	12	112	77.8
T_d	26	5	13	52
O_h	48	10	76	76
I_h	120	10	74	74

Table 4: Point groups (PPS), energy differences between the Franck–Condon S_1 and T_2 states, ΔE_{ST}, and oscillator strengths f between the S_1 and S_0 states.

Molecule	PG	ΔE_{ST} (eV)	f
1	D_{2h}	-0.0251^a	0.0586
1a	D_{2h}	-0.0418	0.6202
1b	C_1	-0.0636	0.6092
1c	C_{2h}	-0.0444	0.6204
2	D_{2h}	0.2552	0.2565
2a	D_{2h}	-0.2475	1.0973
2b	D_{2h}	-0.0834	1.1035
2c	D_{2h}	-0.1482^a	1.2209
2d	D_{2h}	-0.0224	1.3284
2e	D_{2h}	-0.0346	1.3265

[a] The intersystem crossing $T_2 \rightarrow S_1$ is symmetrically forbidden.

Figure Captions

Fig. 1: Schematic representations for the energy diagram of (a) symmetry-controlled thermally activated delayed fluorescence and (b) the inverted singlet-triplet structure. Each of l, m, and n is a certain integer satisfying $m \geq 1$, $n \geq 2$, and $m > l \geq 0$, and k is all the natural numbers satisfying $1 \leq k < n$.

Fig. 2: Structures of anthracene **1** and its derivatives **1a**–**1c** and those of pyrene **2** and its derivatives **2a**–**2e**.

Fig. 3: Energy levels for (a) anthracene, **1** and (b) its derivative, **1a**. The green and orange values indicate the transition dipole moment in atomic units and the one-electron spin-orbit integral in cm^{-1}, respectively.

Fig. 4: Energy levels for anthracene derivatives: (a) **1b** and (b) **1c**. The green and orange values indicate the transition dipole moment in atomic units and the one-electron spin-orbit integral in cm^{-1}, respectively.

Fig. 5: Energy levels for pyrene, **2**. The green and orange values indicate the transition dipole moment in atomic units and the one-electron spin-orbit integral in cm^{-1}, respectively.

Fig. 6: Energy levels for pyrene derivatives: (a) **2a** and (b) **2b**. The green and orange values indicate the transition dipole moment in atomic units and the one-electron spin-orbit integral in cm^{-1}, respectively.

Fig. 7: Energy levels for pyrene derivatives, **2c**. The green and orange values indicate the transition dipole moment in atomic units and the one-electron spin-orbit integral in cm^{-1}, respectively.

Fig. 8: Energy levels for pyrene derivatives: (a) **2d** and (b) **2e**. The green and orange values

indicate the transition dipole moment in atomic units and the one-electron spin-orbit integral in cm^{-1}, respectively.

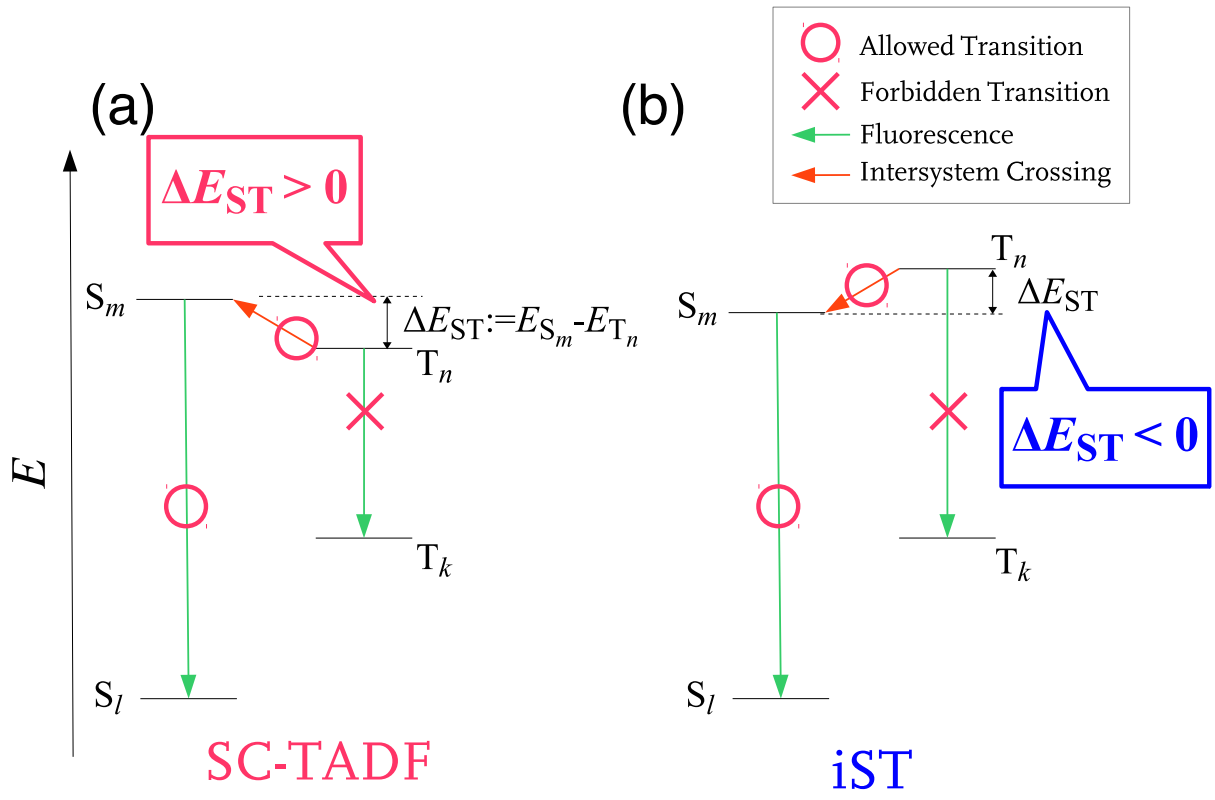

Figure 1: Uejima *et al.*

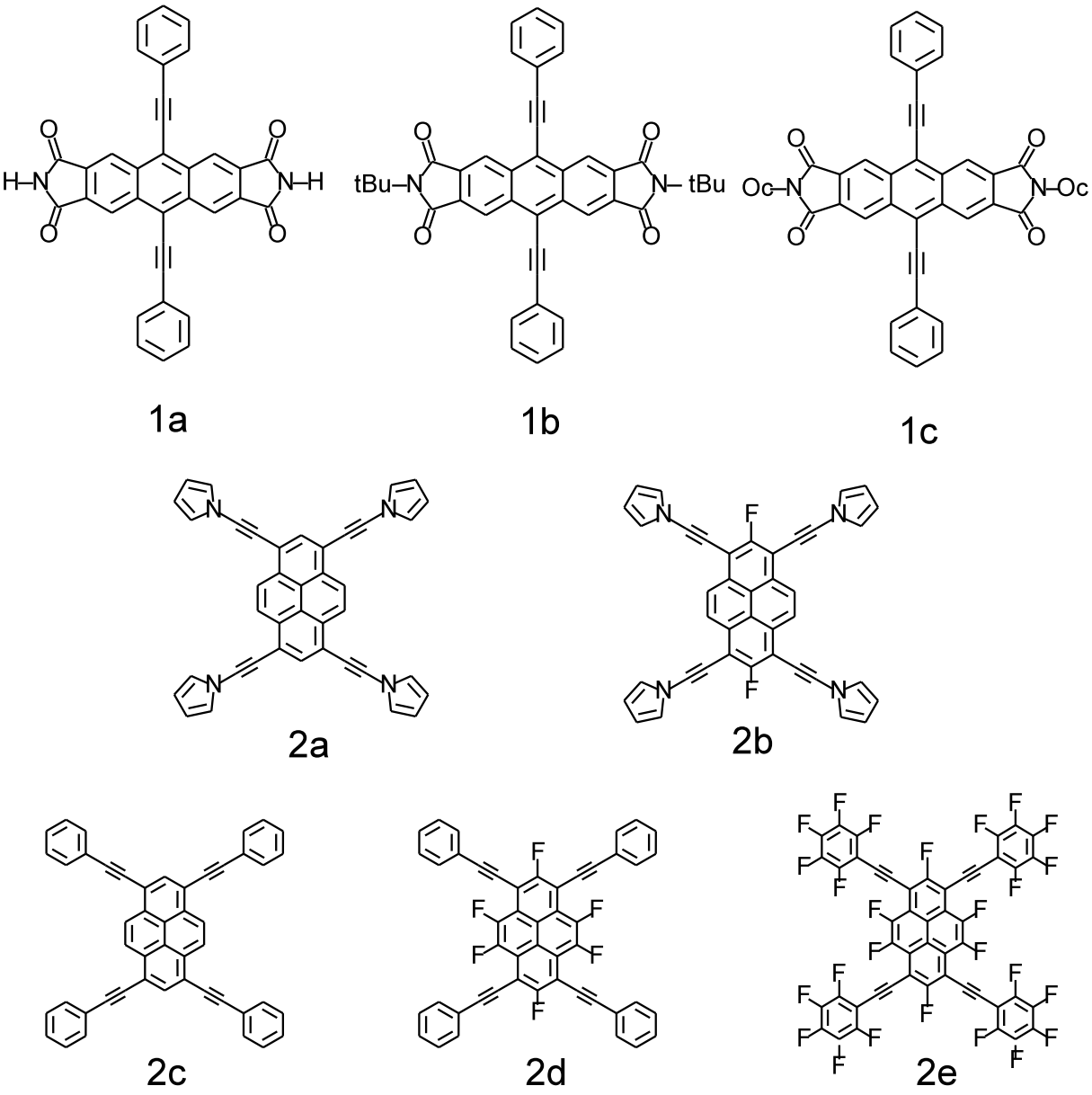

Figure 2: Uejima *et al.*

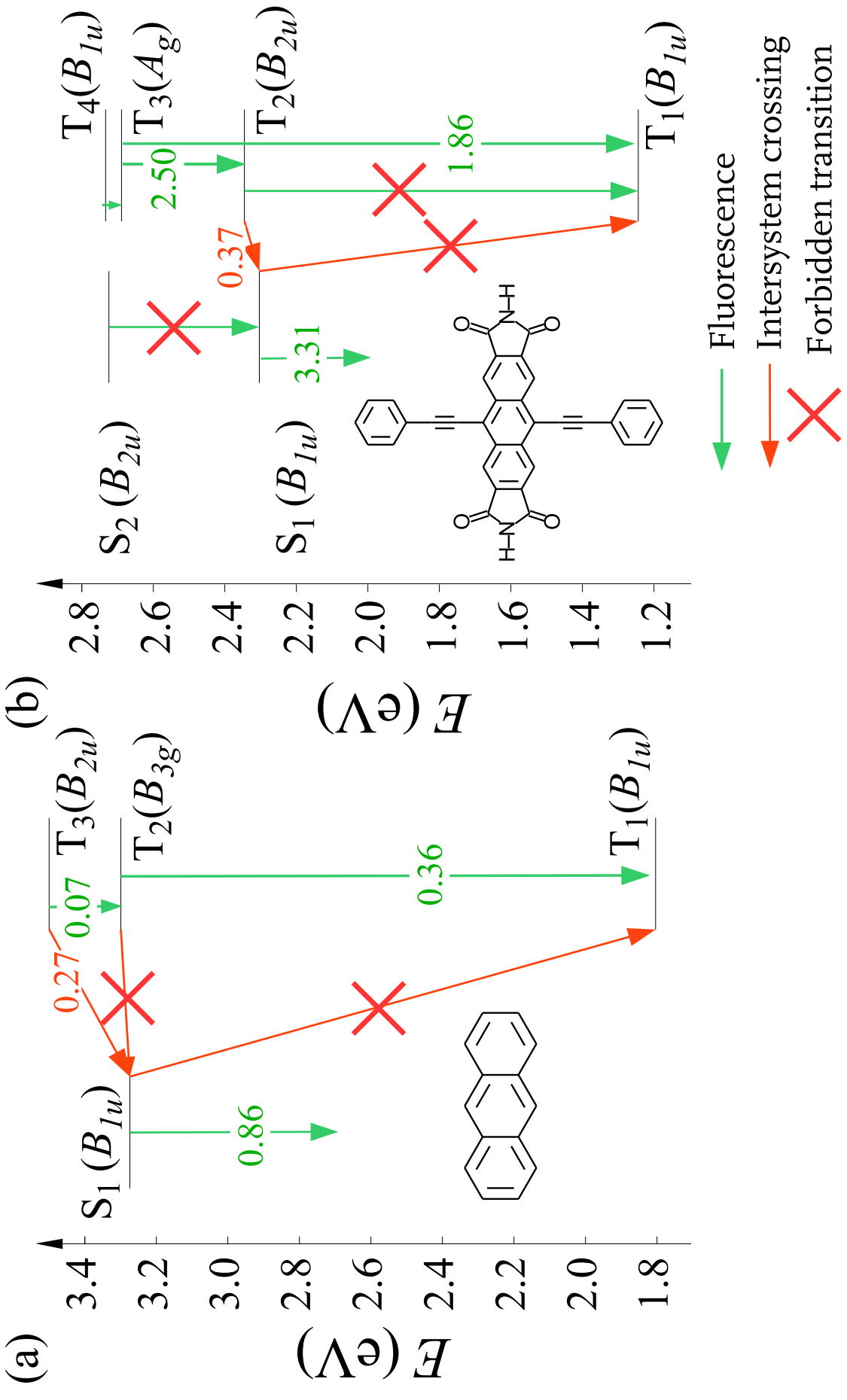

Figure 3: Uejima *et al.*

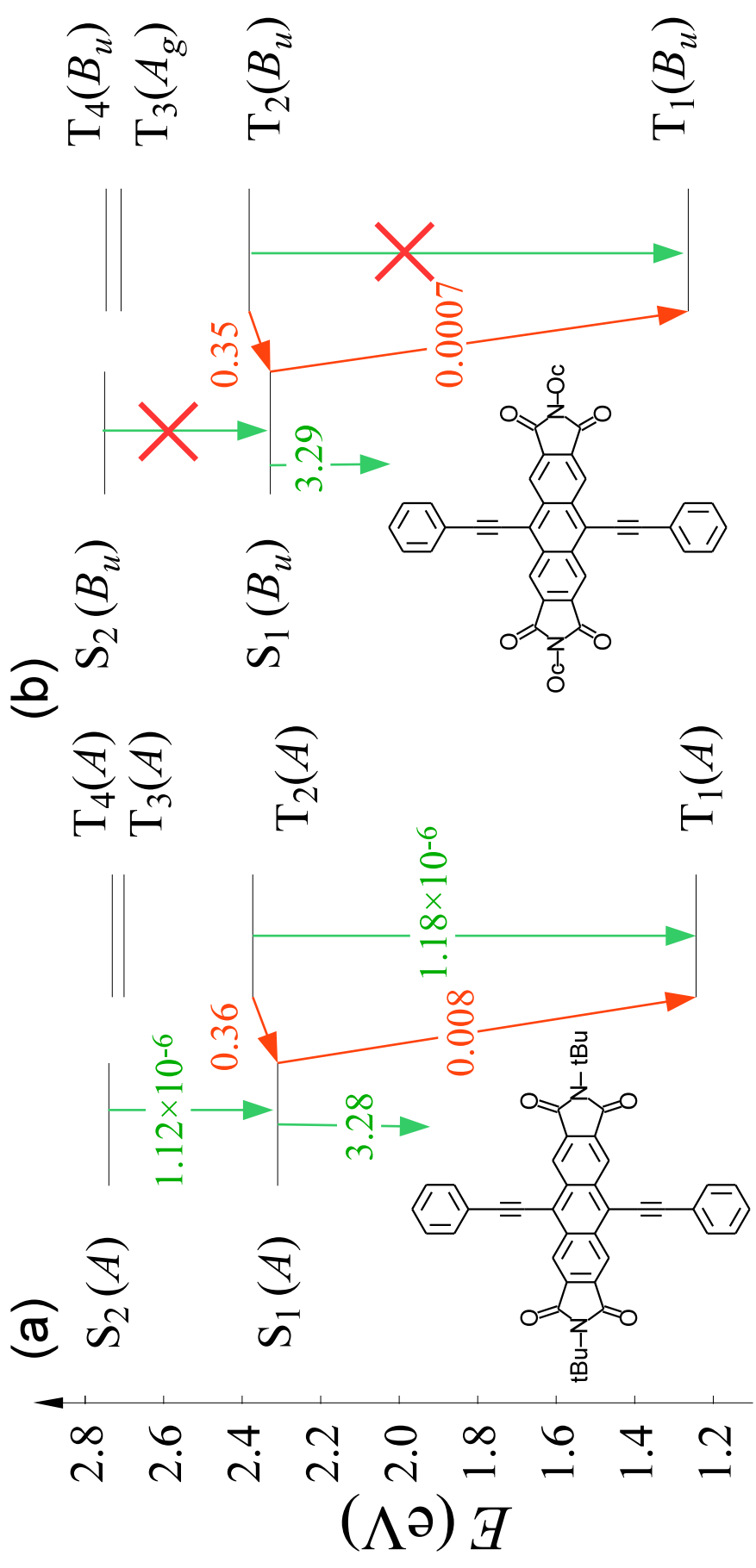

Figure 4: Uejima *et al.*

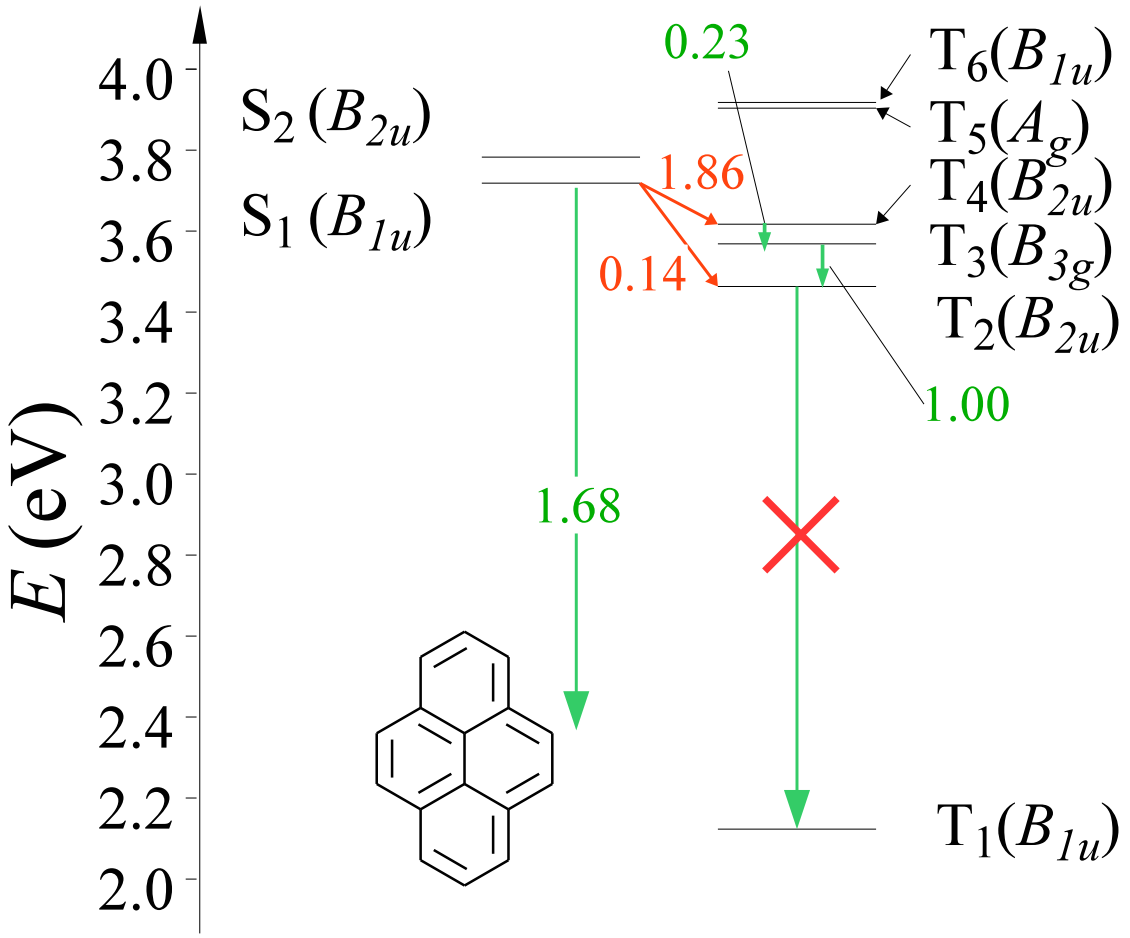

Figure 5: Uejima *et al.*

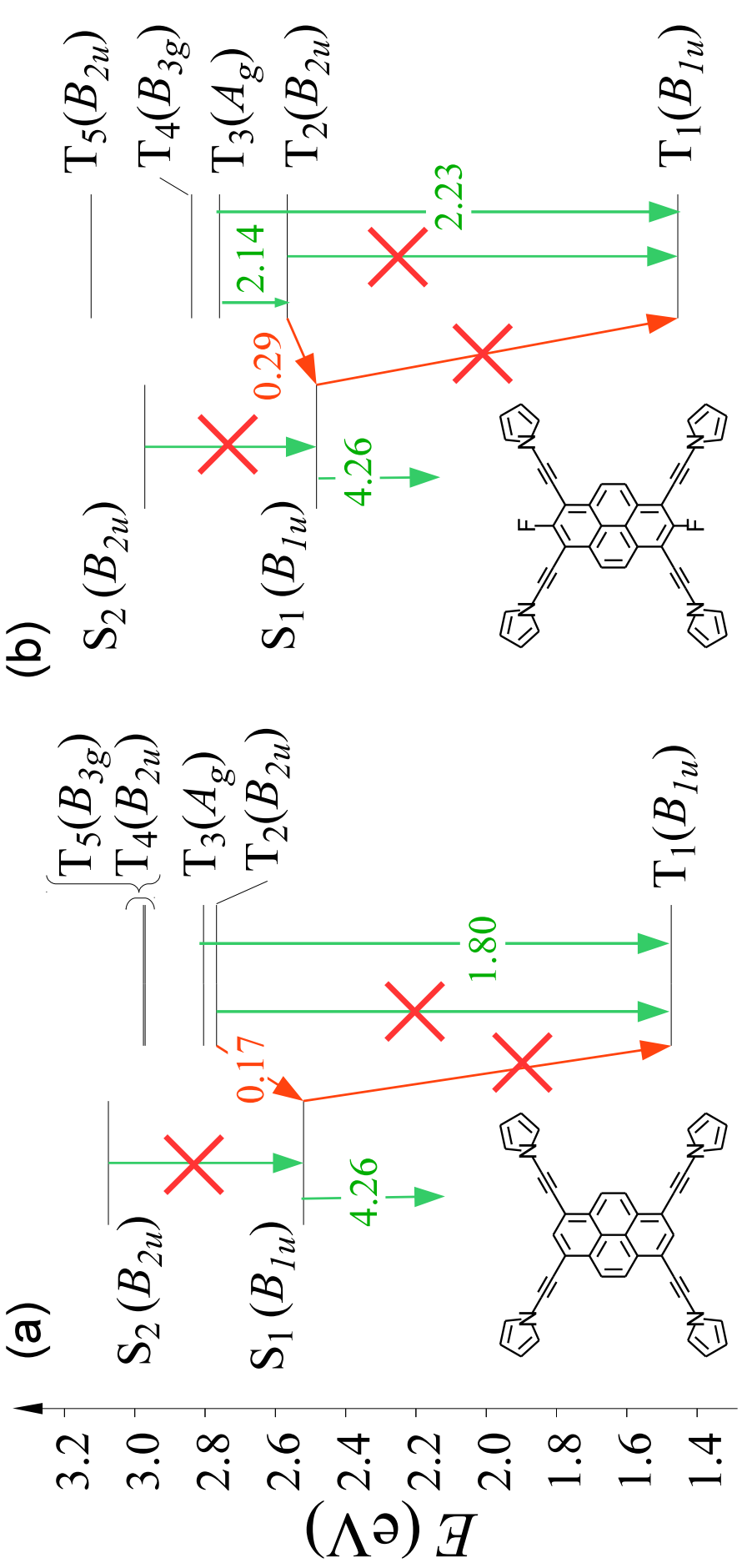

Figure 6: Uejima *et al.*

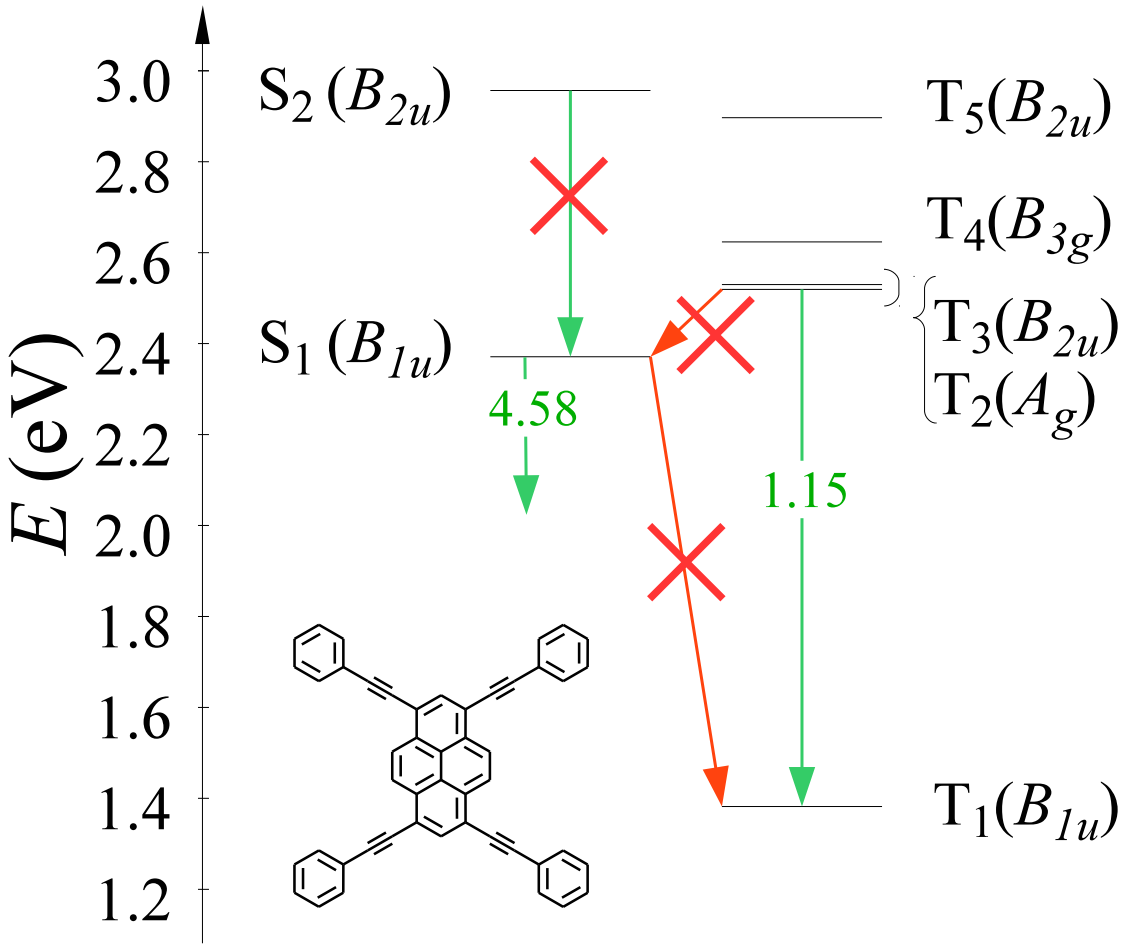

Figure 7: Uejima *et al.*

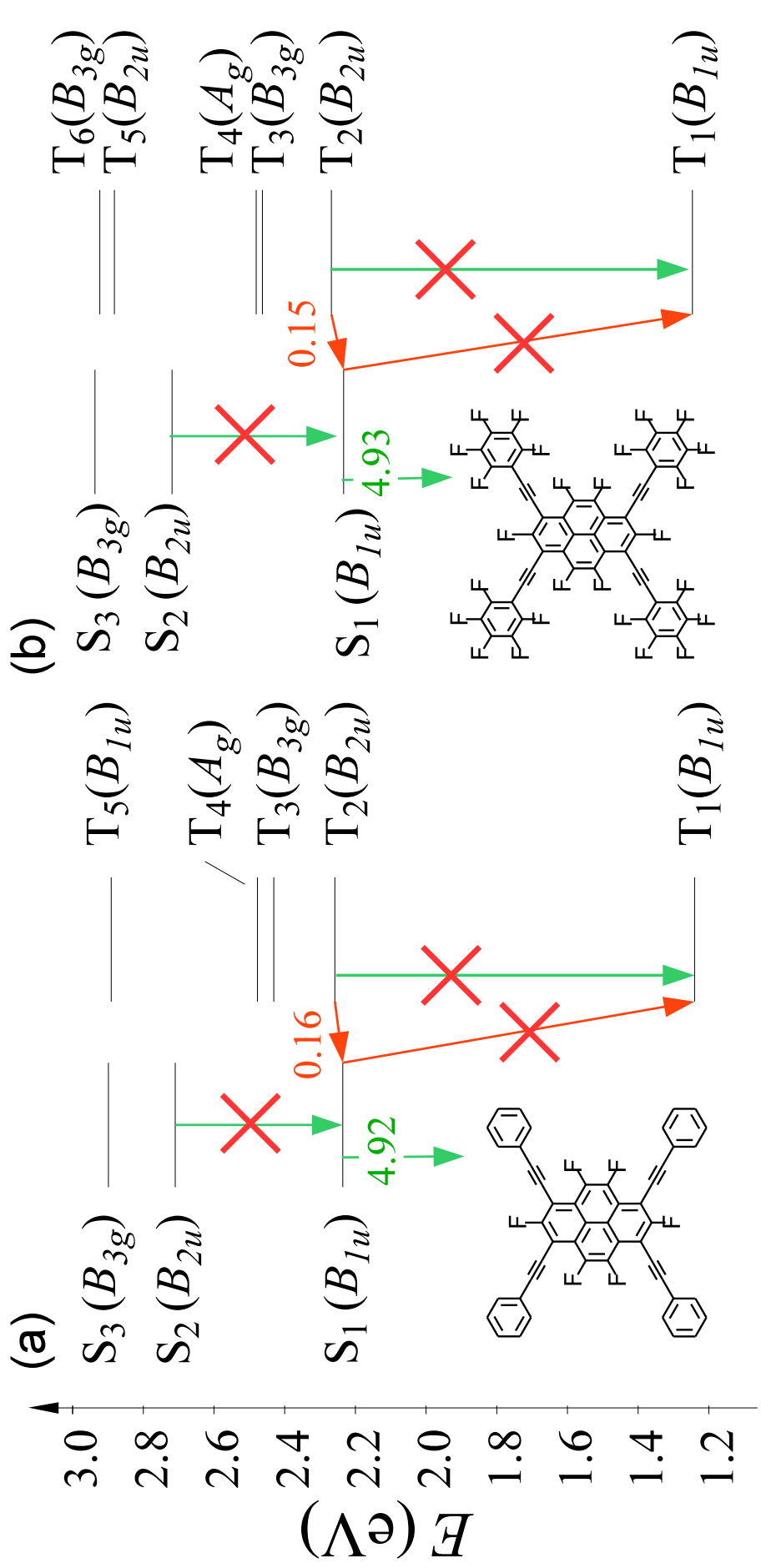

Figure 8: Uejima *et al.*

A graphical and textual abstract for the Table of contents entry

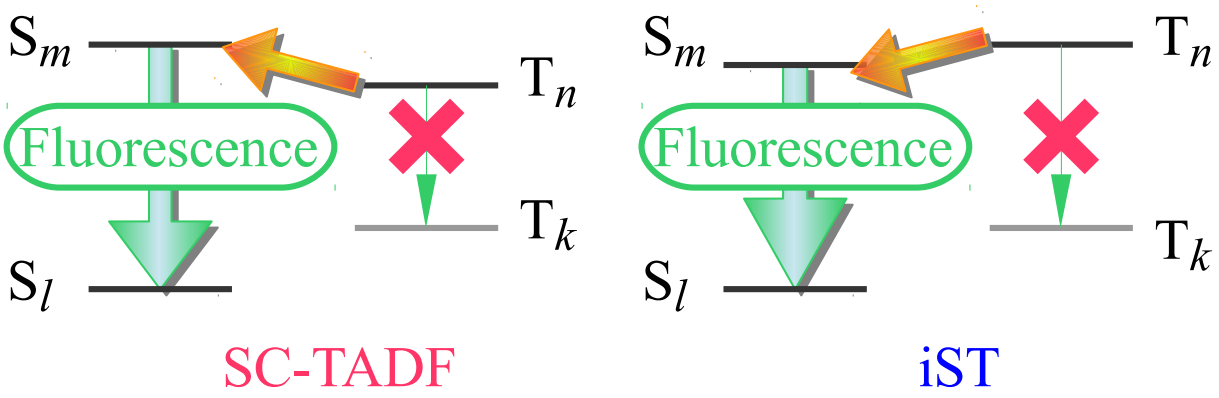

Text: The concepts of symmetry-controlled thermally activated delayed fluorescence (SC-TADF) and inverted singlet-triplet (iST) structure are proposed. SC-TADF or iST molecule can be used as a light-emitting material.